DOI: 10.1002/cbdv.202100096

FULL PAPER

CHEMISTRY & BIODIVERSITY

Cytotoxicity and Antibacterial Evaluation of *O*-Alkylated/Acylated Quinazolin-4-one Schiff Bases

Neha Manhas,[a] Parvesh Singh,*[a] Chunderika Mocktar,[b] Moganavelli Singh,[c] and Neil Koorbanally*[a]

[a] School of Chemistry and Physics, University of KwaZulu-Natal, Private Bag X54001, Durban 4000, South Africa, e-mail: Koorbanally@ukzn.ac.za; singhp4@ukzn.ac.za

[b] Discipline of Pharmaceutical Sciences, School of Health Sciences, University of KwaZulu-Natal, Private Bag X54001, Durban 4000, South Africa

[c] Non-Viral Gene Delivery Laboratory, Discipline of Biochemistry, School of Life Sciences, University of KwaZulu-Natal, Durban 4000, South Africa

A series of quinazolin-4-one Schiff bases were synthesized and tested *in vitro* for their cytotoxicity against two cancerous cell lines (MCF-7, Caco-2) and a human embryonic cell line (HEK-293) including their antibacterial evaluation against two Gram-positive and four Gram-negative bacterial strains. Most of the quinazoline-Schiff bases exhibited potent cytotoxicity against Caco-2. 3-[(*Z*)-({4-[(But-2-yn-1-yl)oxy]phenyl}methylidene)amino]-2-methylquinazolin-4(3*H*)-one (**6f**) with the *O*-butyne functional group displayed three-fold higher cytotoxic activity (IC_{50} = 376.8 μM) as compared to 5-fluorouracil (5-FU; IC_{50} = 1086.1 μM). However, all compounds were found to be toxic to HEK-293, except for 3-[(*Z*)-({4-[(2,4-difluorophenyl)methoxy]phenyl}methylidene)amino]-2-methylquinazolin-4(3*H*)-one (**6h**) that showed ~three-fold lower toxicity and higher selectivity index than 5-FU. Structure–activity relationship (SAR) analysis revealed that *O*-alkylation generally increased the anticancer activity and selectivity of quinazoline-4-one Schiff bases toward Caco-2 cells. The fluorinated Schiff-base generally exhibited even more significant cytotoxic activity compared to their chlorine analogs. Surprisingly, none of the quinazoline-4-one Schiff bases displayed encouraging antibacterial activity against the bacterial strains investigated. Most of the compounds were predicted to show compliance with the Lipinski parameters and ADMET profiles, indicating their drug-like properties.

Keywords: quinazoline-4-one Schiff-bases, anticancer activity, breast cancer, colon cancer, human embryonic cells, ADMET, Lipinski.

Introduction

Over the years, cancer has been one of the leading causes of death globally, with startling figures and statistics published annually by various research agencies. According to the International Agency for Research on Cancer (IARC), cancer is the major cause of morbidity and mortality with approximately 14 million new cases and 8 million cancer related deaths in 2012.[1] The World Health Organization (WHO) also indicated that nearly 1 out of 6 deaths is caused by cancer globally, and that it was responsible for 8.8 million deaths in 2015; thus, globally, the second leading cause of death.[2] In terms of cost, this has had a serious impact on global economies. In the US alone, the total cancer related medical costs in 2013 and 2014 was US $74.8 and $87.8 billion, respectively, while an approximate amount of US $1.16 trillion was estimated in 2010.[3–5] These Figures are expected to rise by 70% in just two decades, with the greatest impact felt by low income countries due to insufficient services catering for cancer patients.

Amongst the five major forms of cancer in women (breast, colorectum, lung, cervix, and stomach), breast cancer is the most commonly diagnosed cancer in women and accounts for 25% of the total cases of

Supporting information for this article is available on the WWW under https://doi.org/10.1002/cbdv.202100096

cancer and the highest cancer related mortality rates in women. Breast cancer accounts for 34% of deaths in Europe and North America.[1] Although this rate is declining in developed countries such as the UK and the US, the situation remains aggressive in developing nations.[6] Closely related to breast cancer in terms of epidemiology is colorectal cancer. It occurs in both men and women and remains the second leading cause of cancer death in both sexes combined.[4] It is the third most diagnosed form of cancer and responsible for 10% of global cancer cases.[7]

Chemotherapy (the use of chemical agents with pharmacological importance) – remains the treatment of choice in combating cancer. Heterocyclic scaffolds can be considered the soul of cancer chemotherapy due to their ubiquity in almost all available anticancer agents. Food and Drug Administration (FDA) survey of 2017 drug approvals in oncology, showed that all drugs approved contain a heterocyclic skeleton.[8]

Quinazolines and its derivatives are an important class of heterocycles in cancer research. Heterocycles has continued to receive significant attention by both synthetic organic and medicinal chemists over the years. For example, the commercially available anticancer drugs; Gefitinib – a reversible epidermal growth factor receptor (EGFR) inhibitor and Afatinib – a dual EGFR-ErbB2 inhibitor, both contain a quinazoline unit in their matrix. The epidermal growth factor receptor (EGFR) is highly expressed in the breast cancer cell lines, MCF-7. It is thus commonly used in anti-breast cancer research. To this effect, quinazolines have been applied with significant success.[9–13] They have also found application as inhibitors of vascular endothelial growth factor (VEGF) receptors, responsible for angiogenesis with a promising IC_{50} of 48 nM reported.[14] In addition, they were studied for their cytotoxicity against colorectal cancer using the Caco-2 cell line,[15] where they induced an acute cytotoxic effect against the cell lines at 149.2 and 74.6 μM.

In the era of multidrug resistant (MDR) tumors, where single target therapy is ineffective in combating the malignant process, molecular hybridization – the combination of two or more pharmacophoric units to create a new hybrid with improved capability of being recognized by multiple receptors – is becoming popular in drug design for anticancer research.[16] The versatility of quinazolines is expressed in this regard, and new molecular hybrids with important pharmacophores such as triazole[17,18] and isatin[19,20] improved cytotoxicity against MCF-7 breast cancer cell lines.

Schiff bases play a vital role in drug design and development due to their chelating ability and high metabolic stability.[21] Derivatives of quinazolines have also demonstrated good activity against the breast cancer cell lines – MCF-7.[14,22,23] Additionally, quinazoline analogs and their Schiff bases showing their potential as antibacterial agents have also been documented in literature.[24,25]

Considering the increasing occurrence of MDR tumors, and in our quest to synthesize new biologically important heterocyclic scaffolds, this study is focused on the synthesis of new quinazolin-4-one Schiff bases and their *in vitro* antiproliferative activity in breast cancer (MCF-7) and colon cancer (Caco-2) cell lines. Finally, the antibacterial screening of these compounds against two Gram-positive and four Gram-negative strains was also undertaken under *in vitro* conditions.

Results and Discussion

Chemistry

The aim of this work was to synthesize a new series of Schiff-bases of quinazoline-4-one. Although the most common and established route for the synthesis of libraries of quinazoline-4-one Schiff bases is to condense the amino group with various aldehydes, we only used *para* hydroxybenzaldehyde and formed ethers with the hydroxy group. As such, the aromatic imine is seen to be a linker between the quinazoline-4-one and the alkyl group forming the ether. To the best of our knowledge, this has not been done previously.

The quinazoline-4-ones were prepared by refluxing a mixture of anthranilic acid **1** and acetic anhydride (**2**), to form the intermediate **3**, followed by the careful addition of hydrazine hydrate, forming the 3-amino-2-methylquinazolin-4-one (**4**). The Schiff base precursor **5** was subsequently synthesized by the condensation of the 3-aminoquinazoline-4-one **4** and 4-hydroxybenzaldehyde in a yield of 75%. No purification was necessary for the quinazoline-4-one Schiff base **5**. The subsequent base promoted reaction of **5** with different alkyl/acyl halides in the presence of a mild inorganic base K_2CO_3, afforded quinazoline-4-one Schiff bases **6** in excellent yields (88–95%) (*Scheme 1*).

The structures of the synthesized compounds were unambiguously assigned on the basis of NMR, IR and HR-MS data. With the help of 2D (HSQC, HMBC and COSY) NMR techniques, the full structure elucidation of all compounds was accomplished. For example, the ^{1}H spectrum of compound **6f**, 3-[(*Z*)-({4-[(but-2-yn-1-yl)oxy]phenyl}methylidene)amino]-2-methylquinazolin-4(3*H*)-one, showed a characteristic quartet (δ 4.73, J= 2.3) for H-11 and a highly shielded triplet (δ 1.87, J=

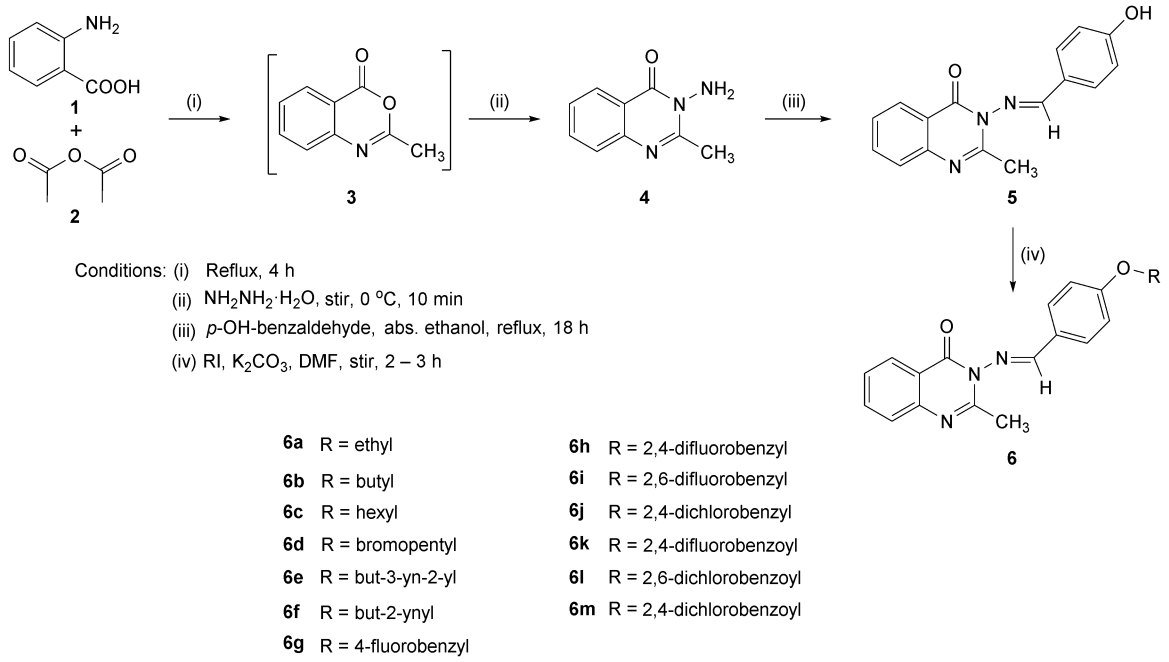

Scheme 1. Synthetic scheme for the preparation of Schiff bases of quinazoline-4(3*H*)-ones.

2.3) for H-14 due long range coupling (^5J) between CH_2-11 and CH_3-14. The aromatic region showed two doublets ($J = 8.8$) at δ 7.07 and δ 7.85 attributed to H3′/H5′ and H2′/H6′, respectively, a double doublet at δ 8.28 ($J = 8.0$, 1.2, H-5) and a doublet at δ 7.66 ($J = 7.8$, H-8). In addition, two triplets of doublets at δ 7.45 ($J = 8.0$, 1.0, H-6) and δ 7.72 ($J = 8.2$, 1.4, H-7) were also present. The most deshielded singlet resonance at δ 8.87 was due to the iminic proton (H-10).

The ^{13}C spectrum of **6f** displayed several characteristic resonances. The acetylene moiety attached to the aromatic ring was characterized by the methylene resonance at δ 56.5 (C-11), two acetylene resonances at δ 73.3 (C-13) and 84.5 (C-12), and a highly shielded methyl resonance at δ 3.6 (C-14). The methyl group attached to the quinazoline-4-one was seen at δ 22.8 (C-2a). The *para* substituted aromatic ring contained two intense resonances at δ 115.3 (C-3′/C-5′) and 130.6 (C-2′/C-6′), while C-5 to C-8 on the quinazoline-4-one ring were present at δ 127.2, 126.3, 134.2 and 126.8, respectively. Four deshielded singlet aromatic resonances attributed to the oxygenated aromatic resonance C-4′, the carbonyl resonance C-4, and two aromatic C–N resonances, C-2 and C-8a were present at δ 161.3, 158.7, 154.0 and 146.5, respectively, while the two more shielded resonances at δ 121.5 and 125.7 were attributed to C-4a and C-1′, two aromatic singlet carbon resonances, respectively. The iminic carbon (C-10) resonated at δ 166.3.

Both C-4 and C-8a showed HMBCs to H-5, and these two resonances were distinguished based on a HMBC from H-7 to C-8a. In a similar manner, C-4a was distinguished from C-1′ by a HMBC to H-6. The two methyl groups were assigned based on HMBCs from H-2a to C-2 and H-14 to C-12. The HMBC between the iminic proton (H-10) and C-2′/6′, allowed C-2′/6′ and C-3′/5′ to be differentiated (*Figure 1*).

Biological Evaluation

Cytotoxicity Studies

All the synthesized compounds were tested *in vitro* for their cytotoxicity against two cancer cell lines, namely

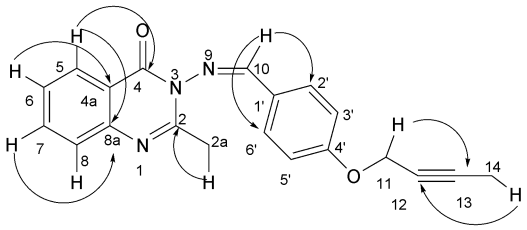

Figure 1. Characteristic HMBC data observed in compound **6f**.

human breast cancer (MCF-7), human colon adenocarcinoma (Caco-2) as well as normal human embryonic cells (HEK-293), using the well-established [3-(4,5-dimethylthiazol-2-yl)-2,5-diphenyltetrazolium bromide (MTT) based cell viability assay. 5-Fluorouracil (5-FU) was used as the reference drug. The samples were dissolved in DMSO to generate different dilutions for the assay. The results are summarized in *Table 1*.

Most quinazoline-4-one Schiff bases displayed cytotoxicity against the colon cancer cell lines (Caco-2). Structure–activity relationship (SAR) analysis revealed that the nature of the different moieties introduced to the basic framework, after *O*-substitution, influenced the cytotoxic effect of the Schiff bases against Caco-2 cells by 1–2 fold. Compound **6f** with an *O*-butyne group exhibited the highest activity (IC_{50} = 376 μM) amongst the tested compounds, comparable to 5-FU, but was 8 fold more toxic than 5-FU against the HEK293 cell lines. The attachment of the same functionality through its secondary carbon (**6e**), dramatically reduced (~three-fold) the cytotoxicity, indicating that a methyl group in the terminal position (as in **6f**) was more desirable for cytotoxic activity.

Compounds with *O*-butyl (**6b**), *O*-hexyl (**6c**), and *O*-bromopentyl (**6d**) substitution also displayed good cytotoxicity against Caco-2, with **6b** having 2.5 fold higher activity than 5-FU, but with greater cytotoxicity. In contrast, the presence of an ethyl functionality dramatically reduced (~seven-fold) the activity of compound **6a** with respect to **6f**, the most active compound of the series. However, *O*-benzylation or *O*-benzoylation did result in more active compounds than 5-FU. Amongst these, **6i** bearing a 2,6-difluorobenzyl moiety exhibited the highest activity with an IC_{50} value of 423.8 μM, whereas **6l** with a 2,6-dichlorobenzoyl moiety emerged as the second most active (IC_{50} = 457.5 μM) compound against the Caco-2 cell lines in this category of compounds.

Table 1. *In vitro* cytotoxic analysis of Schiff bases **6a**–**6m** against two cancer cell lines (Caco-2 and MCF-7) including human embryonic cells (HEK293).

Compound	IC_{50} (μM)			Selectivity Index (Caco-2)
	HEK293	Caco-2	MCF-7	
6a	185.4	2686.3	538.1	0.07
6b	126.5	420.9	NA	0.3
6c	200.7	633.4	NA	0.3
6d	154.6	507.7	NA	0.3
6e	155.9	1048.8	NA	0.1
6f	169.2	376.8	1509.0	0.4
6g	126.8	507.5	NA	0.2
6h	3859.8	1679.2	NA	2.3
6i	96.0	423.8	NA	0.2
6j	98.2	NA	326.0	–
6k	117.8	473.5	779.1	0.2
6l	113.5	457.5	NA	0.2
6m	135.8	707.1	NA	0.2
5-FU	1352.3	1086.1	1057.6	1.2

NA = not active (cell viability < 30 %).

The second potent compound of the series was **6h**, with a 2,4-diflourobenzyl group, which showed almost 3-fold lower toxicity than 5-FU against the normal cell lines. Incidentally, the activity of this compound against the Caco-2 cell lines was almost 1.5-fold lower than 5-FU. However, the relatively better selectivity index (SI) (2.3, *Table 1*) of **6h** outweigh this 1.5 fold decrease in activity. Some important SAR points from these results are: (i) *O*-alkylation generally increases the cytotoxic activity of quinazoline-4-one Schiff bases against Caco-2 cells; (ii) fluorine-containing Schiff bases are generally more potent than their chlorine analogs; and (iii) the quinazoline-4-one ring connected to the phenyl ring *via* an iminic bond is a satisfactory pharmacophore for cytotoxicity against the Caco-2 cell lines.

For breast cancer activity, only four compounds, **6a** (with an ethyl group), **6f** (but-2-ynyl group), **6j** (2,4-dichlorobenzyl group), and **6k** (2,4-difluorobenzoyl group) of the series showed encouraging cytotoxic effects against the MCF-7 cancer cell lines, with IC_{50} values ranging from 326.0 to 1509 μM. All Compounds, except **6f**, displayed superior activity as compared to 5-FU (1057.6 μM). All compounds, however, were found to be more cytotoxic (between 98 and 185.4 μM) than 5-FU (1352.3 μM) against the HEK293 cell lines.

Antibacterial Activity

The synthesized compounds **6a**–**6m** were also screened to determine their antibacterial potential against two Gram-positive strains *viz. Staphylococcus aureus* and MRSA and four Gram-negative strains *viz. Pseudomonas aeruginosa*, *Escherichia coli* (*E. coli*), *Klebsiella pneumonia* and *Salmonella typhimurium*. The disc diffusion method was used for screening these compounds for antimicrobial activity under *in vitro* conditions. All compounds showed no activity against two bacterial strains, *K. pneumonia* and *P. aeruginosa* at a concentration of 10 μg mL^{-1} (not shown in *Table 2*). The Schiff base (**6f**) bearing a butyne moiety exhibited the highest activity against *E. coli* with a zone of inhibition (ZI) value of 12 mm, while three compounds, **6d**, **6e** and **6k** showed moderate anti-

Table 2. *In vitro* antibacterial activity of the synthesized Schiff bases.

No.	*S. aureus*	MRSA	*E. coli*	*S. typhimurium*
6b	–	–	–	7 ± 3.1
6d	–	10 ± 1.5	–	–
6e	–	9 ± 2.1	–	–
6f	–	–	12 ± 1.7	–
6g	–	–	–	7 ± 2.6
6k	7 ± 2.4	11 ± 0.8	–	–
6m	7 ± 1.8	–	–	–

* Only active compounds are included.

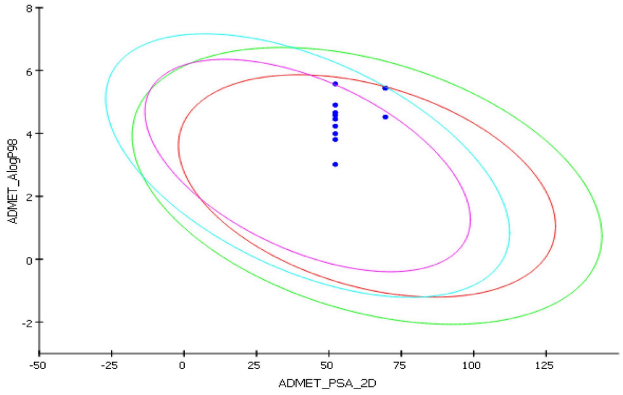

Figure 2. 2D plot between atom-type partition coefficient (ALogP98) and polar surface area (PSA) in Å^2 for all compounds, obtained using DS. The area encompassed by the ellipse is a prediction of good absorption without any ADMET violation.

bacterial activity against MRSA, with zones of inhibition of between 9–11 mm (*Table 2*). Since, none of the compounds displayed any promising activity (zone of inhibition $>$15 mm), no further screening was undertaken.

ADMET Properties and Lipinski's Rule of Five

The absorption, distribution, metabolism, excretion, and toxicity (ADMET) properties of a molecule within a living organism is an in silico prediction that allows for the screening of compounds in the early stage to avoid the synthesis of molecules, which have the potential to be toxic, or metabolized to an inactive form in the body. It also serves as a guide for further structural manipulations to improve the molecule's pharmacokinetics and toxicity.

The pharmacokinetic parameters of our compounds were predicted using six predetermined ADMET models embedded in the Discovery Studio (DS) 4.0 Client (Accelrys, San Diego, CA, USA),[26] and are listed in *Table 3*. A bi-plot (*Figure 2*) obtained between the 2D polar surface area (ADMET_PSA_2D) and the atom-type partition coefficient (ADMET_AlogP98) comprises 99% and 95% confidence space for the prediction of the membrane permeability of the compounds, and corresponds to the Blood Brain Barrier (BBB) and Intestinal Absorption models.[27] The 95% confidence ellipse refers to a region of chemical space where $\geq$95% drug is absorbed, whereas the 99% confidence ellipse represents a region where a substantial amount of the drug is absorbed though the membrane.

Considering that the plasma membrane is capable of forming both hydrophilic and hydrophobic interactions, the optimal drug should have a balance between its hydrophilic and lipophilic character, and can be determined by its polar surface area (PSA), an indicator for hydrogen forming capacity of a molecule and log P (n-octanol-water coefficient) values, respectively. According to the ADMET model, the drug with optimum membrane permeability should have PSA $<$ 140 Å^2 and AlogP98 $<$ 5. Following the AlogP98 criteria, all compounds, except **6j**, **6l** and **6m**, displayed acceptable hydrophobicity ($<$5, *Table 3*), and satisfied the 95% and 99% confidence ellipse for both BBB and human intestinal absorption. All compounds also showed acceptable PSA (52.2 and 69.5) and undefined values for BBB (from −0.18 to −6.8) with the exception of compound **6j** showing a high probability of BBB penetration.

The aqueous solubility plays an important role in the bioavailability of a drug. Accordingly, the two compounds (**6b** and **6f**) found to be most active against the Caco-2 cancer cell lines showed a better solubility profile in comparison to the other compounds. None of the compounds were predicted to be toxic to the liver, based on hepatotoxicity predictions. Moreover, compound **6j** showed no cytochrome P450 2D6 enzyme inhibition, suggesting its optimal metabolism in Phase-1, whereas the false predictions were achieved for the remaining compounds of the series.

In order to determine if the synthesized compounds show compliance to the Lipinski's 'rule of five',[28] their other descriptors were predicted viz. hydrogen bond donors (HBD) and hydrogen bond acceptors (HBA), in addition to their predetermined topological polar surface area (TPSA) and AlogP values. The knowledge of these parameters is again very useful to check the probability of hit molecules to be developed further as drug candidates. As mentioned previously, a TPSA greater than 140 has

Table 3. Predicted ADMET and Lipinski parameters of the compounds **6a**–**6m**.

No.	ADMET solubility	ADMET solubility level	ADMET-CYP2D6 probability	ADMET-CYP2D6	ADMET hepatotoxicity	ADMET AlogP98	ADMET_ PSA_2D	MWt	TPSA	HBA	HBD
6a	−4.161	2	−5.31753	FALSE	0	3.012	52.23	307.3	54.26	4	0
6b	−4.792	2	−5.31763	FALSE	0	3.992	52.23	335.4	54.26	4	0
6c	−5.316	2	−4.74634	FALSE	0	4.905	52.23	363.5	54.26	4	0
6d	−5.026	2	−6.87053	FALSE	0	4.572	52.23	428.3	54.26	4	0
6e	−5.163	2	−3.95266	FALSE	0	4.233	52.23	331.4	54.26	4	0
6f	−4.724	2	−3.30258	FALSE	0	3.805	52.23	331.4	54.26	4	0
6g	−5.389	2	−0.184901	FALSE	0	4.453	52.23	387.4	54.26	4	0
6h	−5.583	2	−2.07184	FALSE	0	4.658	52.23	405.4	54.26	4	0
6i	−5.604	2	−1.7747.3	FALSE	0	4.658	52.23	405.4	54.26	4	0
6j	−6.384	1	0.707771	TRUE	0	5.576	52.23	438.3	54.26	4	0
6k	−5.495	2	−3.1283	FALSE	0	4.523	69.53	419.4	71.33	5	0
6l	−6.319	1	−3.13104	FALSE	0	5.441	69.53	452.3	71.33	5	0
6m	−6.296	1	−2.33313	FALSE	0	5.441	69.53	452.3	71.33	5	0

been associated with the poor bioavailability of drug molecules. Similarly, a HBD greater than five, HBA greater than 10, molecular weight greater than 500 and ClogP greater than five indicates poor absorption/permeation of a drug candidate.

All computations were done employing the 'Filter by Lipinski and Veber Rules' module in DS program. The results are included in *Table 3*. The analysis of computed descriptors denotes that all compounds showed compliance with the Lipinski's rule of five, with the exception of compounds **6j**, **6l** and **6m** showing violation of ClogP (LogP). These results clearly indicate that the majority of compounds have the potential to be developed as drugs with optimal pharmacokinetic properties.

Conclusions

A series of quinazolin-4-one Schiff bases **6a**–**6m** were prepared by a simple base-promoted *O*-alkylation/acylation reaction of 3-{[(4-hydroxyphenyl) methylidene]amino}-2-methylquinazolin-4(3*H*)-one (**5**) with a variety of substituted alkyl and acyl halides. All reactions yielded the final products without complicated purification procedures in excellent yields. Full ^{1}H- and ^{13}C-NMR assignments of all synthesized compounds was documented using 2D NMR techniques. The *in vitro* cytotoxicity screening of these compounds allowed us to identify several potent compounds against the Caco-2 cancer cell lines, where 3-[(*Z*)-({4-[(but-2-yn-1-yl)oxy]phenyl} methylidene)amino]-2-methylquinazolin-4(3*H*)-one (**6f**) showed 3-fold more potent activity than 5-FU. Compound **6h** was found to be less toxic than 5-FU against HEK-293 cells. Generally, *O*-alkylation and introduction of fluorine bearing moieties resulted in more cytotoxic compounds. None of these compounds, however, exhibited good antibacterial activity in their preliminary screening. Hopefully, their coupling with other pharmacophoric units would synergize their antibacterial activity and decrease toxicity against normal cells at the same time. Finally, most of the compounds showed compliance with Lipinski and ADMET parameters *in silico*.

Experimental Section

General

All reagent grade chemical reagents used in this study were purchased from Sigma-Aldrich through Capital

Lab, South Africa. Organic solvents were distilled before use. Kieselgel 60 F_{254} plates purchased from Merck were used to perform thin-layer chromatography. Melting points of all synthesized compounds were determined on a sealed capillary tube in an Electrothermal IA9100 melting point apparatus, and are uncorrected. IR spectra were recorded on a PerkinElmer Spectrum 100 FT-IR spectrometer. NMR analysis was carried out in deuterated chloroform using a Bruker Avance 400-MHz NMR spectrometer (9.4 T; Bruker, Germany), using tetramethylsilane (TMS) as an internal standard. Chemical shifts of the deuterated solvent were 7.24 (^{1}H) and 77.0 (^{13}C), relative to TMS. NMR data was analyzed using Bruker TopSpin 3.1 (2008) software. Chemical shift values were expressed as ppm downfield from TMS and *J* values (coupling constants) are given in Hz. High-resolution mass spectral analysis of all compounds was performed on a Waters Micromax LCT Premier TOF-MS instrument using ~1 ppm concentration of sample.

Synthetic Methods

*Preparation of 3-Amino-2-Methyl-3*H*-Quinazolin-4-one* **(4)**

A mixture of 2-aminobenzoic acid (1 mmol) and acetic anhydride (2 mmol) was refluxed at 140 °C for 3 h. Completion of the reaction and formation of oxazine **3** was monitored by thin layer chromatography (TLC). The reported method for the preparation of **4**[29] involves the isolation of the latter, followed by refluxing with hydrazine hydrate (2 mmol) for 2–3 h. Oxazine **3** was generated *in situ*, excess acetic anhydride evaporated and then reacted with hydrazine hydrate at 5 °C (exothermic reaction), using hexane as a solvent. The purpose of hexane was to facilitate the precipitation of compound after complete addition of hydrazine hydrate. The solid (fluffy buff powder) obtained was filtered and washed with water (2× 10 mL) and then, with hexane (20 mL).

Preparation of 3-{[(4-Hydroxyphenyl)methylidene] amino}-2-Methylquinazolin-4(3H)-one **(5)**

A mixture of **4** (0.01 mmol) and *p*-hydroxybenzaldehye (0.01 mmol) was refluxed in absolute ethanol (30 mL) in the presence of 3–4 drops of glacial acetic acid for a period of 16 h and monitored by TLC. Upon completion, the solvent was removed under vacuum. The solid obtained was filtered and recrystallized using absolute ethanol.

*General Preparation for the Schiff Bases of Quinazoline-4(3*H*)-one* **(6a–6m)**

Activated K_2CO_3 (0.02 mmol) was added in small proportions over a period of 5 min at room temperature (25 °C) to a solution of 3-{[(4-hydroxyphenyl) methylidene]amino}-2-methylquinazolin-4(3*H*)-one (**5**; 0.01 mmol) in dimethylformamide (DMF). The reaction mixture was allowed to stir for another 5 min before addition of alkyl or acyl halides (0.01 mmol) to the reaction mixture at the same temperature, and monitored by TLC. Upon completion, the reaction mixture was poured in crushed ice and left to stand for 30 min. The solid compound obtained was filtered using a Buchner funnel, washed with hexane (20 mL), and recrystallized from absolute ethanol.

All the spectroscopic data of **6a–6m** can be found in the *Supporting Information*.

Antibacterial Screening (Disc Diffusion Method)

Antibacterial screening was undertaken against four Gram-negative strains of bacteria *viz. Pseudomonas aeruginosa* (ATCC 27853), *Escherichia coli* (ATCC 25922), *Klebsiella pneumonia* (ATCC 31488) and *Salmonella typhimurium* ATCC 14026, and two Gram-positive strains *viz. Staphylococcus aureus* (ATCC 25923), and methicillin resistant *Staphylococcus aureus* (MRSA) (ATCC BAA-1683).

All Schiff bases (**6a–6m**) were initially subjected to preliminary antibacterial screening using the disc diffusion assay. The bacterial strains were grown overnight in nutrient broth (Biolab, South Africa) at 37 °C and adjusted to a 0.5 McFarland standard. Mueller-Hinton Agar (MHA) plates were prepared by dissolving agar (38 g) in water (1 L), and pouring it into sterile petri dishes, allowing them to cool and set at room temperature. The different bacterial strains were inoculated onto the agar plates by streaking a swab dipped into the bacterial broth over the surface of the agar. A 5 µL aliquot of the synthesized compounds (1 mg in 1 mL DMSO) was spotted onto 12 mm antibiotic discs and placed in the inoculated MHA plates, which were then incubated for 24 h at 37 °C.

Acknowledgement

The authors would like to thank the Center for High Performance Computing (CHPC) based in Cape Town

for access to computational resources and programs. N.K. thanks the National Research Foundation South Africa for a Competitive Grant for Rated Researchers (Grant No. 118534) and Incentive Funding for Rated Researchers (Grant No. 114817).

Author Contribution Statement

N. M. performed the synthesis and characterization of all compounds and wrote the article. P. S. performed the computer simulations, analyzed the data, and assisted with editing the manuscript. C. M. assisted with the antibacterial screening. M. S. assisted with the cytotoxicity screening. N. K. supervised the entire project, edited the manuscript, and checked the data for scientific correctness.

References

[1] International Agency for Research on Cancer (IARC). World cancer report 2014, Accessed on September 14, 2017.
[2] World Health Organization (WHO). *10 Facts about cancer*, http://www.who.int/features/factfiles/cancer/en/index.html (2017), Accessed on September 8, 2017.
[3] American Cancer Society. *Cancer facts & figures.* (American Cancer Society, 2015), Accessed on September 6, 2018.
[4] American Cancer Society. *Cancer facts & figures.* (American Cancer Society, 2016), Accessed on September 5, 2018.
[5] American Cancer Society. *Cancer facts & figures.* (American Cancer Society, 2017), Accessed on September 10, 2018.
[6] A. K. Dubey, U. Gupta, S. Jain, 'Breast cancer statistics and prediction methodology: a systematic review and analysis', *Asian Pac. J. Cancer Prev.* **2015**, *16*, 4237–4245.
[7] R. L. Siegel, K. D. Miller, S. A. Fedewa, A. Barzia, A. Jemal, D. J. Ahnen, R. G. S. Meester, 'Colorectal cancer statistics', *Ca-Cancer J. Clin.* **2017**, *67*, 177–193.
[8] C. Watch, 2017 FDA Approved Drugs, http://www.centerwatch.com/drug-information/fda-approved-drugs/year (2017), Accessed on September 8, 2017.
[9] V. Chandregowda, A. Kush, G. C. Reddy, 'Synthesis and *In Vitro* antitumor activities of novel 4-anilinoquinazoline derivatives', *Eur. J. Med. Chem.* **2009**, *44*, 3046–3055.
[10] S. A. El-Azab, M. A. Al-Omar, A. A. Abdel-Aziz, N. I. Abdel-Aziz, M. A. El-Sayad, M. A. Aleisa, M. M. Sayed-Ahmed, S. G. Abdel-hamid, 'Design, synthesis and biological evaluation of novel quinazoline derivatives as potential antitumor agents: molecular docking study', *Eur. J. Med. Chem.* **2010**, *45*, 4188–4198.
[11] A. M. Alafeefy, A. E. Ash, 'Design, synthesis and biological evaluation of novel quinazoline derivatives as potential anti-cancer agents', *J. Enzyme Inhib. Med. Chem.* **2012**, *27*, 541–545.
[12] K. M. Amin, M. M. Anwar, M. M. Kamel, E. M. Kassem, S. A. Elseginy, 'Synthesis, cytotoxic evaluation and molecular docking study of novel quinazoline derivatives as PARP-1 inhibitor', *Acta Pol. Pharm.* **2013**, *70*, 833–849.
[13] D. H. Fleita, R. M. Mohareb, O. K. Sakka, 'Antitumor and antileishmanial evaluation of novel heterocycles derived from quinazoline scaffold: a molecular modelling approach', *Med. Chem. Res.* **2013**, *22*, 2207–2221.
[14] A. Ashok, K. Thanukrishnan, H. S. Bhojya Naik, S. Ghosh, '6,7-Dimethoxy-quinazolin-4-yl-amino-nicotinamide derivatives as potent inhibitors of VEGF receptor II', *J. Heterocycl. Chem.* **2017**, *54*, 1723–1728.
[15] S. Jantova, D. Slamenˇová, V. Horváth, P. Rauko, 'Induction of cytotoxicity and ssDNA breaks by 9-bromo-5-morpholino-tetrazolo[1,5-*c*]quinazoline in tumor cells cultured in vitro', *Toxicol. in vitro* **2003**, *17*, 457–463.
[16] N. Kerru, P. Singh, N. Koorbanally, R. Raj, V. Kumar, 'Recent advances (2015 – 2016) in anticancer hybrids', *Eur. J. Med. Chem.* **2017**, *142*, 179–212.
[17] C. Su, X. Liu, 'Synthesis of novel 4(3*H*)-quinazolinones with 1,2,3-triazoles moiety conjugated by Schiff Base', *Asian J. Chem.* **2014**, *26*, 5301–5304.
[18] A. V. Nyuchev, V. F. Otvagin, A. E. Gavryushin, Y. I. Romanenko, O. I. Kofiman, D. V. Belykh, H. G. Schmalz, A. Y. Fedorov, 'Synthesis of chlorin-(arylamino) quinazoline hybrids as models for multifunctional drug development', *Synthesis* **2015**, *47*, 3717–3726.
[19] F. L. Faraj, M. Zahedifard, M. Paydar, C. Y. Looi, N. A. Majid, H. M. Ali, N. Ahmad, N. S. Gwaram, M. A. Abdulla, 'Synthesis, characterization, and anticancer activity of new quinazoline derivatives against MCF-7 cells', *Sci. World J.* **2014**, *4*, 212096–212111.
[20] B. Shi, J. Zhang, S. Cao, M. Gao, P. Ding, Z. Li, J. Liao, X. Xu, 'Synthesis and cytotoxic evaluation of hybrids of indolin-2-one and quinazoline 4-(3*H*)-one linked via carbon-carbon double bond', *J. Chin. Pharm. Sci.* **2014**, *11*, 765–771.
[21] W. Qin, S. Long, M. Panunzio, S. Biondi, 'Schiff bases: A short survey on an evergreen chemistry tool', *Molecules* **2013**, *18*, 12264–12289.
[22] M. Ahmed, R. El-Haggar, 'Synthesis and evaluation of some dibromoquinazoline-sulphonamide hybrids and some Schiff's base analogs for their cytotoxic activity', *Anti-Cancer Agents Med. Chem.* **2017**, *17*, 1563–1569.
[23] M. Fares, W. M. Eldehna, S. M. Abou-Seri, H. A. Abdel-Aziz, M. H. Aly, M. F. Tolba, 'Design, synthesis and *In Vitro* antiproliferative activity of novel isatin-quinazoline hybrids', *Archiv der Pharmazie* **2015**, *348*, 144–154.
[24] K. P. Rakesh, H. K. Kumara, B. J. Ullas, J. Shivakumara, D. C. Gowda, 'Amino acids conjugated quinazolinone-Schiff's bases as potential antimicrobial agents: Synthesis, SAR, and molecular docking studies', *Bioorg. Chem.* **2019**, *90*, 103093.
[25] E. Jafari, M. R. Khajouei, F. Hassanzadeh, G. H. Hakimelahi, G. A. Khodarahmi, 'Quinazolinone and quinazoline derivatives: recent structures with potent antimicrobial and cytotoxic activities', *Res. Pharm. Sci.* **2016**, *11*, 1–14.
[26] BIOVIA, Dassault Systèmes, [Discovery Studio Client], [4.0], San Diego: Dassault ystèmes, [2017].
[27] W. J. Egan, K. M. Merz, J. J. Baldwin, 'Prediction of drug absorption using multivariate statistics', *J. Med. Chem.* **2000**, *43*, 3867–3877.
[28] C. A. Lipinski, F. Lombardo, B. W. Dominy, P. J. Feeney, 'Experimental and computational approaches to estimate

solubility and permeability in drug discovery and development settings', *Adv. Drug Delivery Rev.* **2001**, *46*, 3–26.

[29] D. B. Farag, N. A. Farag, A. Esmat, S. A. Abuelezz, E. Abdel-Salam Ibrahim, A. A. E. E. Dalal, 'Synthesis, 3D pharmacophore, QSAR and docking studies of novel quinazoline derivatives with nitric oxide release moiety as preferential COX-2 inhibitors', *MedChemComm* **2015**, *6*, 283–299.

Received February 6, 2021
Accepted March 15, 2021

